Int J Clin Exp Med 2015;8(5):7015-7028
www.ijcem.com /ISSN:1940-5901/IJCEM0006454

*Original Article*

# Early quantitative CT analysis of oleic acid induced acute respiratory distress syndrome in a canine model

Huai Chen[1], Qing-Si Zeng[1], Rong-Chang Chen[2], Wen Li[3], Jia-Xuan Zhou[1], Qin-Liu[1], Wang-Chun Dai[1]

*[1]Department of Radiology, The First Affiliated Hospital of Guangzhou Medical University, Guangdong 510120, China; [2]National Key Laboratory of Respiratory Diseases, The First Affiliated Hospital of Guangzhou Medical University, Guangdong 510120, China; [3]Nuclear Medicine, Cancer Center of Guangzhou Medical University, Guangdong 510095, China*

Received January 29, 2015; Accepted March 26, 2015; Epub May 15, 2015; Published May 30, 2015

**Abstract:** Background: Although quantitative computed tomography (CT) has been used to analyze the lungs of patients with confirmed diagnoses of acute respiratory distress syndrome (ARDS), there are few reports to show the diagnosis during the early stage of ARDS. Using a canine model and quantitative CT, we aimed to develop an oleic acid (OA) induced ARDS regarding the early stage of ARDS that could improve in the early diagnosis of ARDS. Methods: Fourteen healthy beagle dogs underwent CT. Their lung tissue was manually partitioned into four compartments, i.e., non-aerated, poorly aerated, normally aerated, and hyper-aerated lung compartments. The mean CT attenuation value Hounsfield unit (HU), tissue mass (g), residual volume (ml), and percentage of lung area were automatically determined for each lung compartment and compared between groups by receiver operating characteristic curve (ROC) analyses using area under curve (AUC). The optimized cut-off point for each parameter was determined by Youden's index. Results: Regarding lung compartments during the expiratory phase, the percentage of non-aerated lung area in the ARDS group was higher vs. controls at all time points (T1 to T6). CT attenuation values for the ARDS group increased with time during both respiratory phases compared with controls. During both respiratory phases, tissue mass within the ARDS group significantly increased compared with controls at T3-T6. Conclusions: Quantitative CT analysis can detect ARDS at an early stage with high sensitivity and specificity, providing a minimum of assistance in the early diagnosis of ARDS.

**Keywords:** Acute respiratory distress syndrome, computed tomography, quantitative analysis, canine model, attenuation value, Hounsfield unit

## Introduction

Acute respiratory distress syndrome (ADRS) is a common critical illness with a mortality rate of 40-60%. The main reason for the high mortality rate usually stems from the severity of the inciting insult leading to the ARDS the cause for high mortality. Even once the diagnosis is made, the mortality rate remains elevated at 38.5-40% [1]. Previous studies have shown that blood gas analysis (the "gold standard" for the diagnosis of ARDS) usually lags behind pulmonary pathologic changes [2]. In addition, X-ray manifestations also lag by approximately 4-24 h behind the clinical manifestations [2, 3].

In the mid 1990's, measurement of the positive end-expiratory pressure (PEEP)-induced alveolar air volume was used to determine the reduction in the computed tomography (CT) value of the non-aerated lung parenchyma at a certain level. Generally, the level was a single CT slice close to the diaphragmatic surface, and the measured CT values were between -100 and 100 HU. This approach ignored the alveolar CT attenuation characteristics in the poorly aerated areas (with CT values between -100 HU and 500 HU) [4]. Therefore, the PEEP-induced alveolar air volume was often underestimated. In addition, estimations based on CT values from a single slice can underestimate or overestimate the alveolar air volume throughout the entire lung. Therefore, a new CT method was developed using scans which included the entire lung from apex to diaphragm. When the end-expiratory lung volume was equal to the

functional residual capacity (FRC), the image obtained was considered zero end expiratory pressure (ZEEP). PEEP occurred using 35 cm $H_2O$, whereby end-expiratory and end-inspiratory CT images were obtained [5].

A significant advancement was achieved when pulmonary quantitative CT was proposed as a tool to determine the potential for lung recruitment (thus optimizing the setting of PEEP) [6, 7] and to assess lung hyperinflation in an effort to reduce the occurrence of ventilator-induced lung injury [6-9]. Quantitative pulmonary CT is a sensitive method used to discern changes in the volume, density, and mass of pulmonary lesions and can accurately reflect density changes of lung tissue in the area of the lesion [4-10].

Using quantitative CT to analyze the lungs of patients with confirmed diagnoses of ARDS, researchers have found that the "weight" of the lungs is approximately 2-3 times that of normal lung, and the volume of air in the lungs is significantly reduced [11]. As far we knew, quantitative CT has not been used to study the early stages of ARDS. Several quantitative CT parameters may be interesting and useful as early parameters in diagnosis of ARDS, particularly percentages of aerated vs. non-aerated and poorly aerated lung area, as well as mean CT attenuation value (HU) and tissue mass (g). The aim of this study was to analyze canine models of oleic acid induced ARDS regarding the early stage of ARDS that could improve in the early diagnosis of ARDS.

## Materials and methods

### *Experimental animals*

Beagle dogs (n = 14) with an average age 3.0 ± 1.4 years and weighing 10.8 ± 2.9 kg were provided by Guangzhou Institute of Pharmaceutical Industry. The study was approved by Medical Ethics Committee of Guangzhou Medical College. The dogs were randomly divided into two groups, the experimental group (n = 10) and the control group (n = 4). A ventilator (EVITA 4 Germany) was used to control each dog's breathing. The oxygen concentration was set at 50%, the ventilator inspiratory-to-expiratory time ratio was 1:2 and the respiratory rate was 25-40 times/min [12].

Although rabbits, sheep, goats, and pigs have been used previously in animal models of ARDS [5, 13], we chose beagle dogs because their body size is larger than rabbits and, thus, their lung size is closer to that of humans. Also, since they are smaller than sheep, goats, and pigs, they are more manageable.

### *Anesthesia and surgical preparation*

Dogs were fasted for 12 h before each experiment and drinking water was not allowed during fasts.

Anesthesia was divided into two stages. For the first stage, or induction phase, anesthesia was induced using an intramuscular injection of 0.2 mg/kg body weight of ketamine, 10 mg midazolam, and 0.25 mg atropine, and laryngoscope-guided endotracheal tube (ETT) intubation (ETT inner diameter: 7.5 mm) was performed to maintain the breathing passage of each animal.

The right femoral vein was punctured and a guide wire was inserted to lead a Swan Ganz catheter (Edwards LifeSciences; Irvine, California) into the intrathecal space, which was used to anesthetize animal, monitor changes in pulmonary artery wedge pressure (PCWP) before and after treatment, and prepared for all oleic acid injections. A 4F pulse contour continuous cardiac output (CCO) [PiCCO] catheter was placed in the left femoral artery (using the same method adopted on the right side) to monitor arterial blood pressure, core temperature, and extravascular lung water and also to collect specimens for arterial blood gas analysis (i-STAT Abbott, Illinois) to monitor changes in $PaO_2/FiO_2$ before and after treatment.

The second stage, or maintenance phase of anesthesia, aimed at ensuring that the dog remained anesthetized throughout the experiment. To accomplish this, 5-10 mg/kg/h propofol and vecuronium 0.25-0.5 mg/kg/h (push-needle pump SN-50C6, Shenzhen) were injected continuously via the central venous catheter. Central venous access was established to ensure a patent access for anesthesia, and infusions during the experiment. A continuous intravenous (IV) infusion of normal saline at 50 ml/h was administered via the central venous catheter and diluted heparin solution was used to flush the IV line intermittently to maintain line patency.

At the cessation of the experiment (at the T6 time point), all dogs were euthanized by propofol overdose injection and the basal segment of the lower lung was harvested for pathological analysis.

*Construction of ARDS model*

The ARDS model was constructed by injecting the experimental group with 0.18 ml/kg oleic acid (Sigma-Aldrich, St. Louis, MO, USA) within 30 min. The value of 0.18 ml/kg of oleic acid was based on previous established criteria, with which the final concentration of oleic acids is equivalent to 0.08 mg/kg in dog [12, 14]. In the controls, oleic acid was replaced with 0.18 ml/kg saline using the identical injection method. The oleic acid was injected into the right femoral vein to reach the right atrium of dog at supine position via Swan Ganz catheter. The Swan Ganz catheter was used for all oleic acid injections and PCWP measurements as it is a long catheter whose proximal tip can be manipulated to enter either the right atrium or pulmonary artery, i.e., it can be readily adjusted according to the requirements of the experiment. When measuring PCWP, the proximal tip is placed within the pulmonary artery, and after the measurement, the proximal tip can be pulled back to the right atrium to avoid pulmonary thrombosis. Animals in both groups were subsequently scanned in the supine position.

*Blood gas analysis*

The 4F PiCCO catheter was used to collect specimens for arterial blood gas analysis to monitor changes in $PaO_2/FiO_2$ before and after treatment. Baseline data were collected before injection of oleic acid in each experiment. The baseline status before model construction was recorded as T0. Thirty min after injection of oleic acid, arterial blood was collected once every 10 min (T1 through T6 every 10 min, sequentially for a total of 60 min based on our experimental design). T6 was the end point collection for blood gas analysis. The total of 90 min (30 min wait time after injection of oleic acid and then 60 min for arterial blood collection) was for our experimental design.

*CT scan parameters*

A Siemens 128-slice spiral CT scanner was used throughout the study. Each dog was scanned from the lung apex to the diaphragmatic dome. The specific scan parameters were: slice thickness: 128 × 0.6 mm; scan speed: 0.5 s/r; field of view (FOV): 180 mm; tube voltage: 120 kV; tube current: automatic (CT scanner was set to automatic tube current, usually 35 mAs); pitch: 1.2; pixel size: 0.32\0.32; acquisition matrix: 512 × 512. A slice interval and thickness of 2 mm were used for reconstruction of the raw data.

A CT scan was performed during both expiratory and inspiratory phases. A total of 0.1 ml vecuronium was injected to block the dogs' spontaneous breathing, and that phase was considered the expiratory phase. To capture the expiratory phase CT images, we not only gave muscle relaxants, but also disconnected the ventilator so that during the expiratory phase acquisition, each dog was not connected to the ventilator, i.e., the dog's airway was directly vented to the atmosphere. After the completion of the expiratory CT images, we reconnected each dog to the ventilator to ensure that oxygen was provided to the dogs. In other words, immediately following the expiratory phase, dogs were given oxygen at 35 cm $H_2O$ pressure using the ventilator, and that phase was considered the end-inspiratory phase.

After modeling, scanning at various sequential time points was denoted by T1, T2, T3, T4, T5, and T6 until the dogs reached ARDS at T6 (T1 through T6 occurred every 10 min; T6 was the end point). Protti et al., [5] in a porcine model, used a PEEP of 45 cmH2O. In our current study, the PEEP was reduced to 35 cm $H_2O$ as dogs have lower body weights compared to pigs.

*Post processing of images*

The CT images from each acquisition (both expiratory and inspiratory phases) were analyzed using pulmonary function analysis software (LungCAD, Neusoft Neusoft Corporation, Shenyang, China). The lung tissue to be analyzed was manually selected and partitioned by Hounsfield units (HU) into one of four regions: [4, 15]: 1, non-aerated lung compartment (CT attenuation values between -100~100 HU); 2, poorly aerated lungs compartment (CT values between -500~-101 HU); 3, normally aerated lung compartment (CT values between -900~-501 HU); and 4, hyper-aerated lung compartment (CT values between -1000~-901 HU). The lung function analysis software automatically

**Table 1.** Changes in $PaO_2/FiO_2$ and PCWP before and after treatment

| | | ARDS | Control | *P*-value |
|---|---|---|---|---|
| $PaO_2/FiO_2$ (mmHg) | Before | 446.68 (27.05) | 486.94 (29.46) | 0.030 |
| | After | 164.08 (21.13)* | 480.75 (34.5) | < 0.001 |
| PCWP (mmHg) | Before | 12.60 (2.32) | 11.50 (1.29) | 0.395 |
| | After | 12.80 (2.49) | 9.50 (1.29) | 0.029 |

Data are presented by mean and standard deviation. *Indicates significant changes compared to baseline within group.

analyzed the mean CT attenuation value of the lung (HU) in the FOV, as well as the tissue mass (g), and the residual lung volume (ml).

All CT scan and post CT images processing were done by a single radiologist (first author), who had more than 20 years experiences.

*Statistical analysis*

Due to budget constraints, only 15 dogs were initially enrolled in the study without *a priori* sample size calculations. The animals were sorted by their weights into 5 blocks with 3 dogs in each block. The first and third dogs of each block were assigned, in sequence, to the experimental group; the second dog in each block was assigned to the control group. One dog in the control group died before completion of the experiment. There was no preexisting illness in others in the experimental group. Finally, four dogs made up the control group and 10 dogs comprised the experimental group.

Quantitative CT analysis and blood gas analysis measurements were expressed as mean ± SD. Two independent sample t-tests were performed to compare differences between ARDS and control sgroups. Once a significant difference between the two groups was observed, the corresponding measurements were further evaluated by receiver operating characteristic curve (ROC) analysis, a graphical plot that illustrates the diagnostic ability to distinguish ARDS status. Area under the ROC curve (AUC), ranging from 0.5 to 1, was used as an indicator of diagnostic performance; higher value of AUC indicates better diagnostic performance (0.85-1.0 indicates high accuracy). Statistical testing as to whether AUC equals to 0.5 (i.e., no discrimination) was also performed. The optimal cut-off point for each parameter was determined by the maximum value of Youden's index, defined by sensitivity + specificity. Due to the small sample size, the estimated AUC was based on a nonparametric assumption. A two-tailed *p* value < 0.05 was considered statistically significant. Statistical analyses were performed using SPSS 15.0 (SPSS Inc., Chicago, IL, US) statistical software.

## Results

*Blood gas analysis*

Before oleic acid treatment, a small but significant difference in $PaO_2/FiO_2$ (446.68 vs. 486.94, P = 0.030) was observed between ARDS vs. control groups. After treatment, significantly lower $PaO_2/FiO_2$ (164.08 vs. 480.75, P < 0.001) and higher PCWP (12.80 vs. 9.50, P = 0.029) were observed in the ARDS group vs. controls, respectively (**Table 1**).

*Quantitative CT analysis*

*Normally aerated lung area:* During the expiratory phase, the percentage of normally aerated lung area decreased with time in both groups. Notably, the percentage of normally aerated lung area was significantly lower in the ARDS animal model vs. controls at T3 (66.32% vs. 80.93%, P = 0.047; Supplemental Table 1; **Figure 1A**, left hand figure).

During the inspiratory phase, the percentage of normally aerated lung area was initially increased in the ARDS group vs. controls at peak time points, T3 and T2, respectively, and then gradually decreased until T6 for both groups. The percentage of normally aerated lung area in the ARDS animals was generally higher than controls and the difference was significant at T3 (68.75% vs. 50.48%, P = 0.018; Supplemental Table 1) (**Figure 1A**, right hand figure).

*Non-aerated lung area:* During the expiratory phase, the percentage of non-aerated lung area in the ARDS group was higher vs. controls and the difference was significant at all time points above baseline, i.e., T1 to T6 (*p*-values: 0.004~0.047; Supplemental Table 1; **Figure 1B**, left hand figure).

For the inspiratory phase, the percentage of non-aerated lung area in both groups was stable and no significant difference was observed

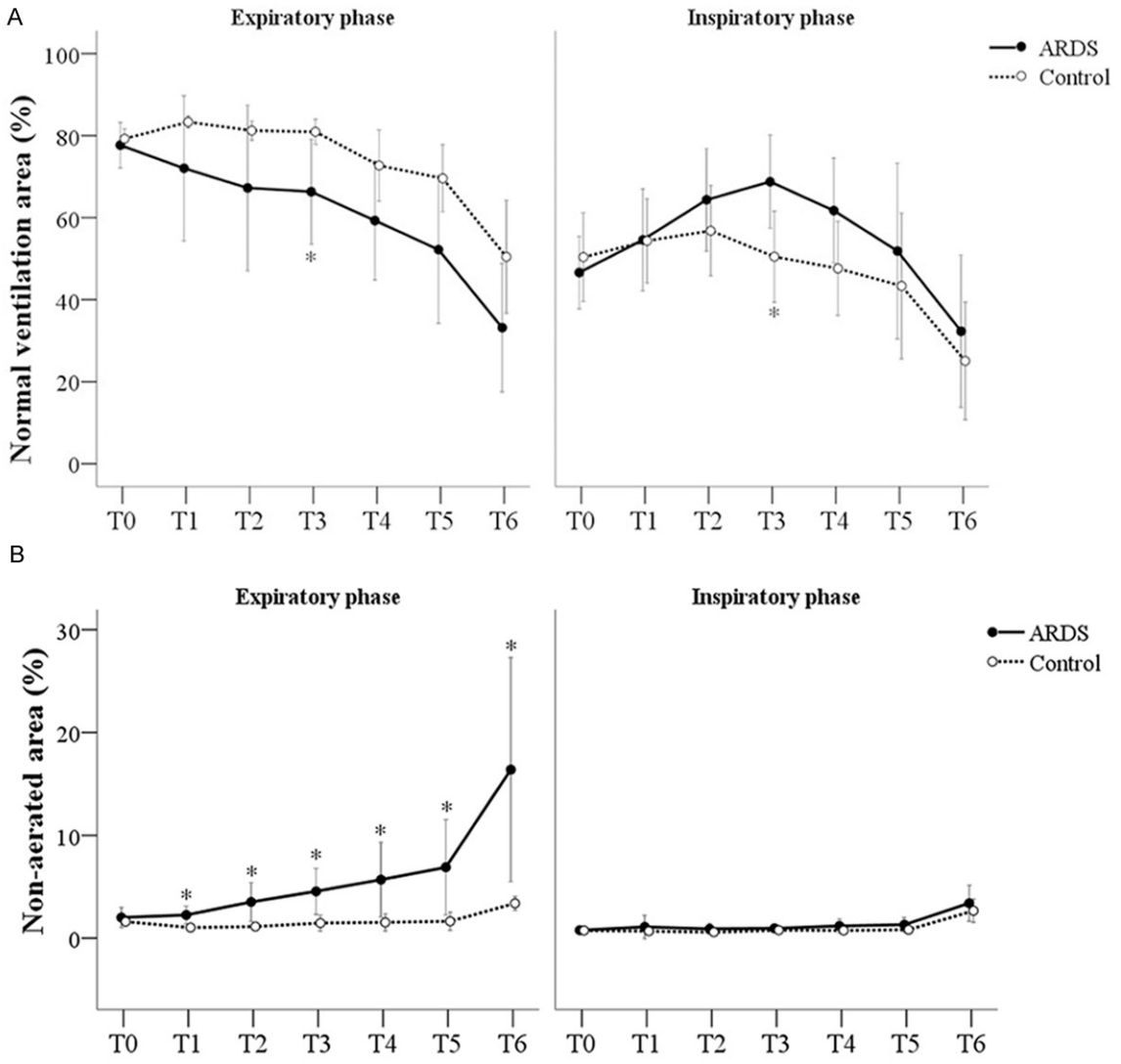


**Figure 1.** Measurements of normally aerated area (A) and non-aerated lung area (B) over time from quantitative CT analysis. Each dot with error bar indicates the mean and standard deviation. *Indicates a significant increase or decrease is observed in ARDS group compared with control group.

between groups at any time point (Supplemental Table 1, **Figure 1B**, right hand figure).

*Poorly aerated area:* During the expiratory phase, the percentage of poorly aerated lung area in both groups increased over time. However, the percentage of poorly aerated lung area in the ARDS group was higher compared with controls and the difference was significant at T3 (23.76% vs. 11.32%, P = 0.034) and T5 (28.98% vs. 15.23%, P = 0.045), respectively (Supplemental Table 1; **Figure 2A**, left hand figure).

During the inspiratory phase, the percentage of poorly aerated lung area in both groups was slightly increased but no significant difference was observed between groups at any time point except T5 (4.36% vs. 2.75%, P = 0.04; Supplemental Table 1; **Figure 2A**, right hand figure).

*Hyper-aerated lung area:* During the expiratory phase, the percentage of hyper-aerated lung area in both groups was stable with no significant difference between groups at any time point (**Figure 2B**, left hand figure).

For the inspiratory phase, however, the percentage of hyper-aerated lung area in the ARDS group decreased initially to its lowest value at T4 and then gradually increased from T4 to T6.

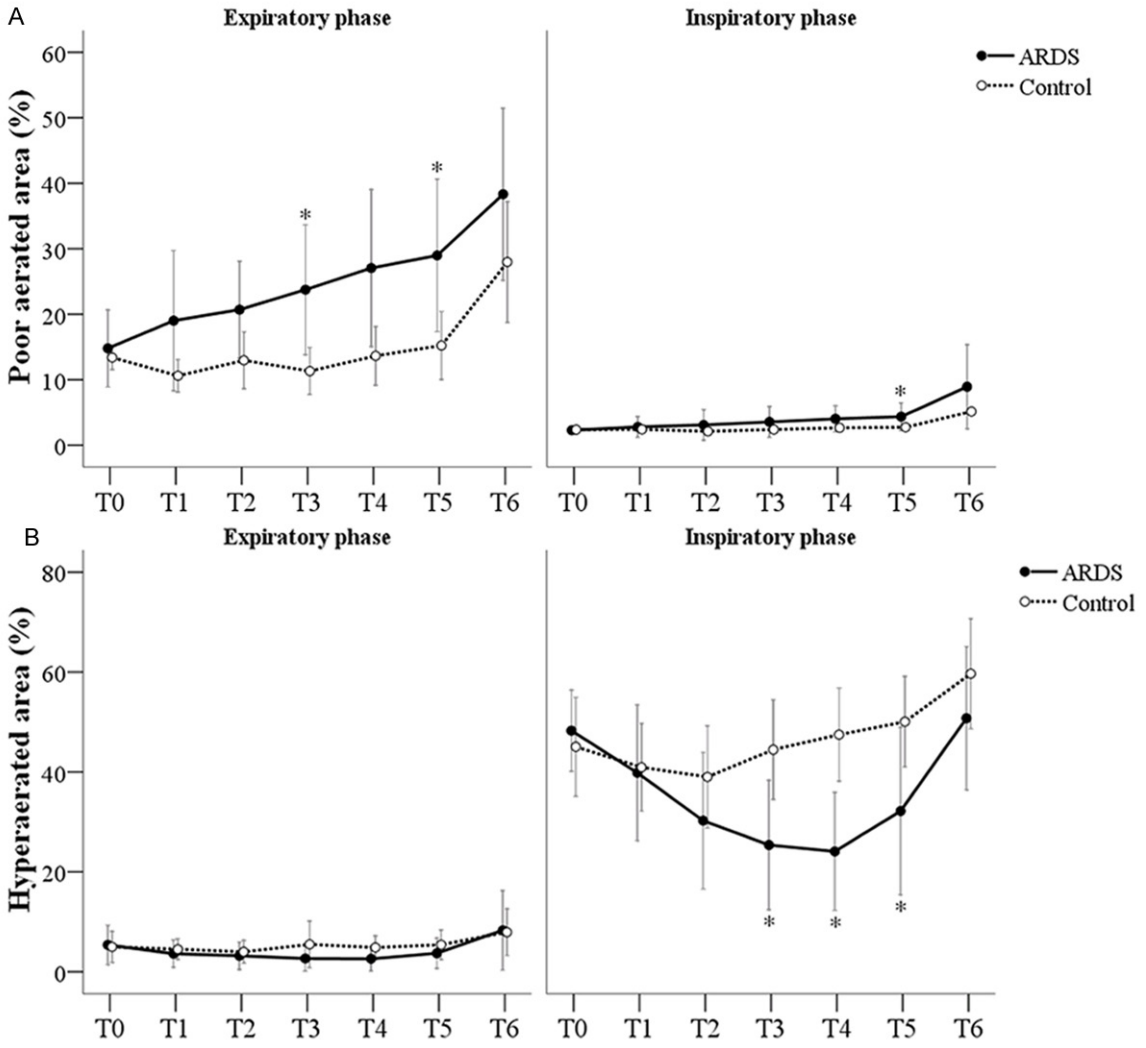


**Figure 2.** Measurements of poorly aerated lung area (A) and hyperaerated lung area (B) over time from quantitative computed tomography analysis. Each dot with error bar indicates the mean and standard deviation. *Indicates a significant increase or decrease is observed in ARDS group compared with control group.

The percentage of hyper-aerated lung area in the ARDS group was lower compared with controls and the difference was significant at T3 (25.38% vs. 44.46%, P = 0.022), T4 (24.10% vs. 47.47%, P = 0.004), and T5 (32.17% vs. 50.07%, P = 0.027), respectively (Supplemental Table 1; **Figure 2B**, right hand figure).

*CT attenuation values*

CT attenuation values (in HU) for the ARDS group increased with time during both expiratory and inspiratory phases compared with controls (whose values were relatively stable during two phases) (Supplemental Table 1; **Figure 3A**).

Significant differences between groups were observed during the inspiratory phase at T6 (-659.63 vs. -750.37, P = 0.024) and during the expiratory phase at T4 (-538.19 vs. -670.23, P = 0.042), T5 (-507.42 vs. -675.07, P = 0.020), and T6 (-391.35 vs. -627.48, P = 0.000), respectively (**Figure 3A**, left hand figure).

*Residual volume*

Residual volumes were stable in both treatment groups during both phases of respiration. There was no significant difference observed between the two groups at any time point during the two phases (**Figure 3B**).

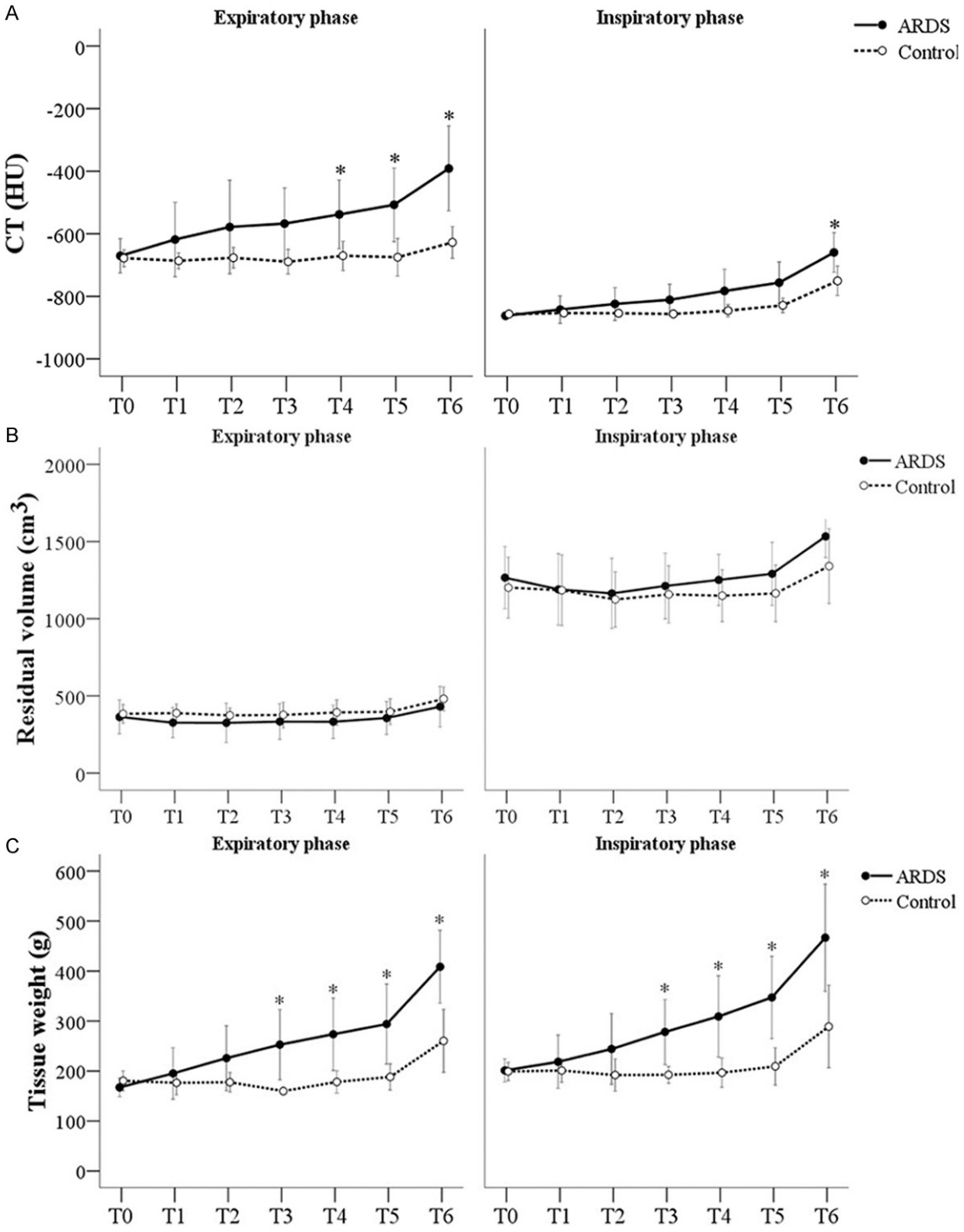


**Figure 3.** Measurements of CT attenuation (A), residual volume (B), and tissue weight (C) over time from quantitative CT analysis. Each dot with error bar indicates the mean and standard deviation. *Indicates a significant increase or decrease is observed in ARDS group compared to control group.

*Tissue mass*

The changes in tissue mass during expiratory and inspiratory phases were similar. During both respiratory phases, tissue mass within the ARDS group significantly increased compared with controls at T3 (252.80 g vs. 159.82 g, P = 0.024 for expiratory phase; 278.12 g vs.

**Table 2.** Statistical evaluation of the diagnostic values of quantitative CT analysis

| Item | Phase | Time | AUC (95% CI) | Cut off point† | Sen. (%) | Spe. (%) |
|---|---|---|---|---|---|---|
| Normally aerated area (%) | exp | T3 | 1.000 (1.000, 1.000)* | < 77.27 | 100 | 100 |
| | insp | T3 | 0.875 (0.670, 1.080)* | > 55.12 | 90 | 75 |
| Non-aerated area (%) | exp | T3 | 0.950 (0.832, 1.068)* | > 2.7 | 80 | 100 |
| | exp | T4 | 0.950 (0.832, 1.068)* | > 3.46 | 80 | 100 |
| | exp | T5 | 0.950 (0.832, 1.068)* | > 3.62 | 80 | 100 |
| | exp | T6 | 1.000 (1.000, 1.000)* | > 4.425 | 100 | 100 |
| Poorly aerated area (%) | exp | T3 | 0.950 (0.835, 1.065)* | > 14.96 | 90 | 100 |
| | exp | T5 | 0.925 (0.767, 1.083)* | > 17.165 | 100 | 75 |
| | insp | T3 | 0.750 (0.484, 1.016) | > 3.125 | 60 | 100 |
| Hyper-aerated area (%) | insp | T3 | 0.875 (0.670, 1.080)* | < 40.06 | 90 | 75 |
| | insp | T4 | 0.975 (0.900, 1.050)* | < 33.71 | 90 | 100 |
| | insp | T5 | 0.850 (0.632, 1.068)* | < 37.455 | 60 | 100 |
| CT value | exp | T1 | 0.825 (0.602, 1.048) | ≥ 650.25 | 70 | 100 |
| | exp | T2 | 0.925 (0.774, 1.076)* | ≥ 642.8 | 90 | 100 |
| | exp | T3 | 0.925 (0.774, 1.076)* | ≥ 647.085 | 90 | 100 |
| | exp | T4 | 1.000 (1.000, 1.000)* | ≥ 633.345 | 100 | 100 |
| | exp | T5 | 1.000 (1.000, 1.000)* | ≥ 626.94 | 100 | 100 |
| | expi | T6 | 1.000 (1.000, 1.000)* | ≥ 563.11 | 100 | 100 |
| Tissue mass | exp | T3 | 1.000 (1.000, 1.000)* | > 183.95 | 100 | 100 |
| | exp | T4 | 1.000 (1.000, 1.000)* | > 206.355 | 100 | 100 |
| | exp | T5 | 1.000 (1.000, 1.000)* | > 224.525 | 100 | 100 |
| | exp | T6 | 0.950 (0.832, 1.068)* | > 355.655 | 80 | 100 |
| | insp | T3 | 1.000 (1.000, 1.000)* | > 219.245 | 100 | 100 |
| | insp | T4 | 1.000 (1.000, 1.000)* | > 234.12 | 100 | 100 |
| | insp | T5 | 1.000 (1.000, 1.000)* | > 259.155 | 100 | 100 |
| | insp | T6 | 0.900 (0.730, 1.070)* | > 370.69 | 80 | 100 |

Exp = expiratory; insp = inspiratory; Sen. = sensitivity; Spe. = specificity. *P < 0.05 for AUC significantly higher than 0.5. †The cut-off values were determined by the maximum value of Youden's index.

192.42 g, P = 0.003 for inspiratory phase), T4 (273.46 g vs. 178.19 g, P = 0.026 for expiratory phase; 309.11 g vs. 196.72 g, P = 0.021 for inspiratory phase), T5 (293.88 g vs. 188.26 g, P = 0.026 for expiratory phase; 347.15 g vs. 209.41 g, P = 0.008 for inspiratory phase), and T6 (408.51 g vs. 260.41 g, P = 0.004 for expiratory phase; 466.60 g vs. 288.93 g, P = 0.012 for inspiratory phase), respectively (Supplemental Table 1, **Figure 3C**).

*ROC analysis of quantitative CT values*

ROC analyses of the quantitative CT measurements for those with significant differences between ARDS and control groups were summarized in **Table 2**. Area under the ROC curve (AUCs) for all quantitative CT measurements were estimated at least 0.85 and were significantly higher than 0.5, except for percentage of poorly aerated area during the inspiratory phase at T3 (AUC = 0.75, P = 0.157) and CT value during the expiratory phase at T1 (AUC = 0.825, P = 0.066).

At T3, the percentage of non-aerated lung area had good diagnostic ability in expiratory phase (AUC = 0.950, sensitivity = 80%, specificity = 100%). Similar results were found in the percentage of hyper-aerated lung area in the inspiratory phase; furthermore, the discrimination ability improved at T4 (AUC = 0.975, sensitivity = 90%, specificity = 100%). In addition, AUCs of tissue mass during the expiratory and inspiratory phase at T3-T6 achieved 0.90 or higher, with sensitivities and specificities reaching 80-100% when using optimized cut-off points of tissue mass to diagnose ARDS. AUCs of CT

**Table 3.** Statistical evaluation of the diagnostic values from blood gas analysis

| Item | AUC (95% CI) | Cut off point† | Sen. (%) | Spe. (%) |
|---|---|---|---|---|
| Weight of empty container (g) | 0.788 (0.505, 1.070) | 7.855 | 100 | 50 |
| Weight of wet lung and empty container (g) | 0.750 (0.490, 1.010) | 32.92 | 70 | 100 |
| Weight of dry lung and empty container (g) | 0.900 (0.714, 1.086)* | 12.7 | 90 | 100 |
| Wet to dry weight ratio of lung (W/D) | 1.000 (1.000, 1.000)* | 5.525 | 100 | 100 |
| $PaO_2/FiO_2$ after treatment | 1.000 (1.000, 1.000)* | 318.48 | 100 | 100 |
| PCWP after treatment | 0.863 (0.667, 1.058)* | 12 | 70 | 100 |

Sen. = sensitivity; Spe. = specificity. *P < 0.05 for AUC significantly higher than 0.5. †The cut-off values were determined by the maximum value of Youden's index.

values in expiratory phase at T4-T6 were 1.0, and the sensitivities and specificities reached 100% when using the optimized cut-off points of CT values to diagnose ARDS (**Table 2**).

Furthermore, the clinical indices for both $PaO_2/FiO_2$ and wet to dry (W/D) weight ratio of lung after treatment indicated high diagnostic accuracy of quantitative CT analysis of ARDS (AUC = 1.000, sensitivity = 100%, specificity = 100% for both measurements; **Table 3**).

## Discussion

The novelty of this study involved the manner whereby pulmonary injury can be detected during the early stage of ARDS using quantitative CT analysis. Our canine model was sensitive to changes in percentage of non-aerated lung at an early stage, which overall reduction in aerated lung volume is a very common ARDS findings in humans [16-19]. Using lung compartments during the expiratory phase, we found that the percentage of non-aerated lung area in the ARDS group was higher vs. controls at all time points above baseline. The percentage of poorly ventilated lung area in the ARDS group was also higher compared with controls at T3 and T5 (both $P < 0.05$). Compared with controls, CT attenuation values for the ARDS group also increased with time during both respiratory phases. Tissue mass within the ARDS group also significantly increased compared with controls at T3-T6 during both respiratory phases. The AUCs for tissue mass at T3-T5 during both respiratory phases equaled 1.000 and sensitivities and specificities reached 100%. In addition, after oleic acid treatment, significantly lower $PaO_2/FiO_2$ and higher PCWP (**Table 1**) were observed in our ARDS group vs. controls, respectively.

*Advantages and disadvantages of using an oleic acid injury (OAI) model*

Ideally, animal models of the early phase of ARDS should reproduce the mechanisms and sequelae that are operative in humans, including the pathological changes that occur. However, no single animal model can reproduce all of the characteristics of the early phase of ARDS in humans, as most models are based on, at most, two methods of injury and most models target a primary tissue, whereas, the primary target tissue in human ARDS remains unknown [20].

In the case of the oleic acid injury (OAI) model, the primary target tissue is the alveolar endothelium. As oleic acid represents approximately 50% of the total fatty acids present in pulmonary emboli in patients after long bone trauma [20, 21], the oleic acid model was developed in an attempt to reproduce early ARDS due to lipid embolism [20, 22].

In this study, we focused on the early stage of ARDS using a canine OAI model to provide new indicators to guide early diagnosis of ARDS. We chose this particular model as it has similar histopathological features to human ARDS during the acute phase including early and rapidly reversible patchy inflammatory lung injury with permeability changes and impairment in gas exchange [20].

Oleic acid instillation provides an excellent model to study these histopathological changes as shown in a canine study by Derks and Jakobovitz-Derks [23, 24]. In six to twelve hours after OA injection, the canine lungs showed alveolar flooding, capillary congestion, hemorrhage and septal necrosis. A more recent study

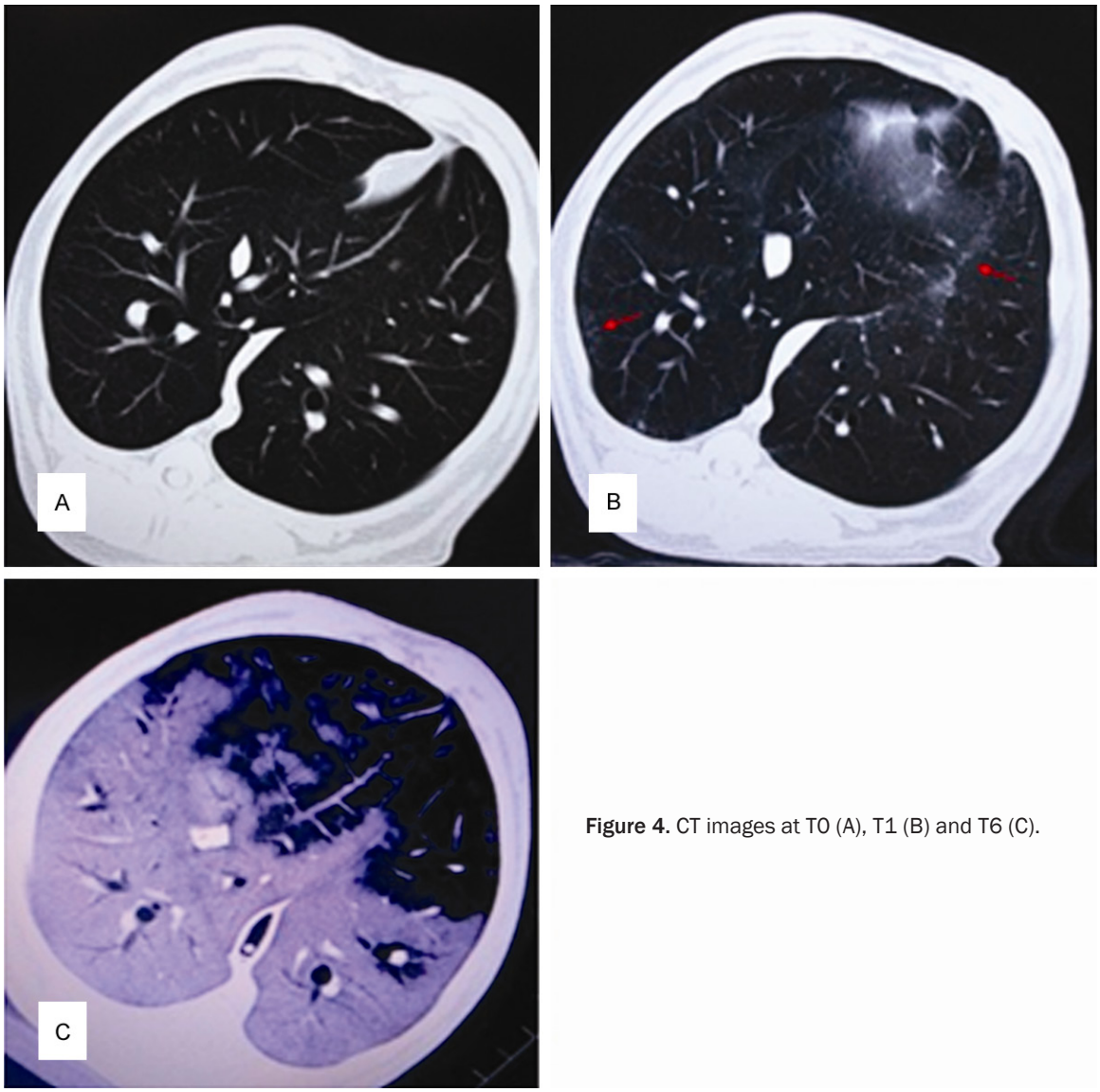


**Figure 4.** CT images at T0 (A), T1 (B) and T6 (C).

has confirmed that the OAI model mimics well the pathological features of ARDS in humans [22, 23]. On microscopic examination, Schuster found interstitial edema, intra-alveolar edema and hemorrhage, and vascular congestion. Hyaline membranes and thrombi in smaller vessels were also occasionally noted [22].

Another major advantage of this model is its ability to reproduce pulmonary injury in different animals. A major disadvantage of the OAI model, however, lies in the fact that few cases of ARDS are associated with long bone trauma or lipid injury [20, 25], and there is no evidence that the pathophysiology of the injury caused by oleic acid (direct toxicity to endothelial cells) is similar to that underlying ARDS associated with sepsis and aspiration. Therefore, the oleic acid model is probably not as appropriate for studying the pathophysiology of ARDS due to sepsis [20].

*Quantitative CT analysis avoids the subjectivity encountered when reading films*

Lung volume is calculated based on the total number of voxels in a given area of interest. Normal lung consists of both air and tissue. The volume of air vs. tissue is calculated according to the close association between the CT attenuation value and the physical density of the lung tissue. The CT number characterizing each individual voxel is defined as the attenuation coefficient of the X-ray by the material being

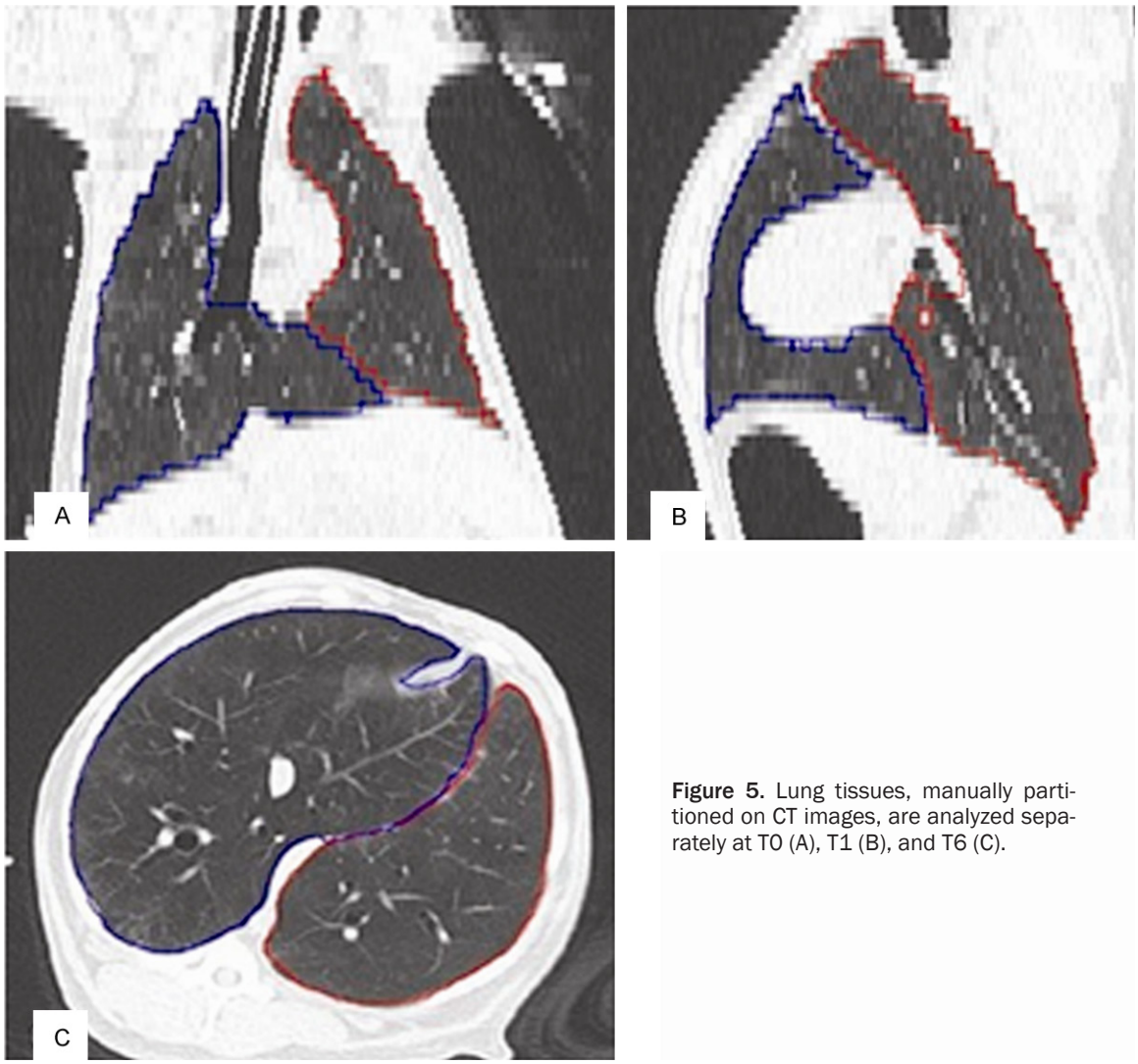


**Figure 5.** Lung tissues, manually partitioned on CT images, are analyzed separately at T0 (A), T1 (B), and T6 (C).

studied minus the attenuation coefficient of water divided by the attenuation coefficient of water, expressed in HU.

By convention, the CT number of water is 0 HU and lung tissue is assumed to have a density very close to the density of water. The CT number is scaled by a factor of 1000 with the CT number of gas being -1000 HU. For example, a lung area characterized by a mean CT number of -200 HU is considered as being composed of 20% of gas and 80% of tissue [16]. The total lung volume, air and tissue volume, air composition, and tissue mass are then calculated using specific software [26, 27], avoiding the subjectivity encountered when reading films.

CT attenuation values for the ARDS group increased with time during both respiratory phases compared with controls. Significant differences were observed between ARDS vs. controls during the inspiratory phase at T6 and during the expiratory phase at T4, T5, and T6, respectively. Funama et al. showed a value of -650 HU for their simulated ground glass opacity (GGO) nodules in their phantom study [28]. In addition, in a study by Lederer et al., high attenuation areas in the lung fields on cardiac CT scans had attenuation values between -600 and -250 Hounsfield units, reflecting ground-glass and reticular abnormalities [29].

This reduction in lung volume has two causative mechanisms: an increase in lung weight (or increase in tissue mass) and a passive collapse of the lower lobes associated with an upward shift of the diaphragm related to muscle paralysis and an increase in intra-abdomi-

nal pressure from anesthesia [30]. As a consequence, PEEP-induced alveolar recruitment predominates in the nondependent cephalad lung regions [30], which can be substantiated by several methods [31, 32].

In the lower lobes of our ARDS dogs, the loss of aeration and increase in lung tissue mass, as shown in **Figure 4** (where ground glass opacities predominated), argues for a common mechanism active in the ARDS dogs involving an upward shift of the diaphragm and increased lung and cardiac weights [27] exerting a direct mechanical compression on the lower lobes [16]. Physiologically, the most caudal, dependent parts of the lung are the lower lobes which are subjected to a lower trans-pulmonary pressure compared to the most cephalic, nondependent upper lobes. In critically ill patients with ARDS, several factors contribute to an exaggeration of these physiological gradients including increased lung weight [18], increased abdominal pressure following abdominal surgery, upward shift of the diaphragm due to anesthesia and paralysis [33] and increased heart weight [16, 27].

Our study had several limitations. Besides the limitations inherent in a canine OAI model, our sample numbers were small (i.e., only 14 animals) and there were no *a priori* sample size determinations. We had no explanations that there were baseline significant difference between the experimental and control groups pre study in blood gas values. Also, the current work is based on the 1994 ARDS definition. An expert panel recently revisited the American-European Consensus Conference definition and released the Berlin definition of ARDS [34, 35]. However, the authors focused only on the ARDS Severity Score published by Rouby et al [36]. Another major limitation is that the study was interrupted before the development of full blown ARDS. No other experiments with other time delays to decide that the 90 minute experiment was optimal. Moreover, no regional analysis of lung data was presented. Additional shortcomings were noted regarding the lung function analysis software used to calculate the lung volume percentages. When the lung function analysis software automatically processed the images, the region of interest was determined by CT attenuation values. If during the experiment, a large amount of exudate and/or consolidation exceeded the region of interest, the software automatically excluded some lung tissue or included some chest wall or mediastinum in the region of interest, resulting in a deviation in the experimental results. To offset this problem, manual partitioning was used (**Figure 5**). Although the manual delineation was performed by the same person, absolute accuracy on the part of a single individual could not assured. Other imaging methods in the future to assess the lung function of the models, including CT perfusion scanning and dual-energy imaging by Dual-source CT, were warranted to investigate.

In conclusion, our canine model, which was based on quantitative CT analysis, changes was observed in percentage of non-aerated lung at an early stage of OA induced ARDS. Quantitative CT parameters, particularly percentages of non-aerated lung area, as well as mean CT attenuation values and tissue mass, are a minimum of assistance in the early diagnosis of ARDS.

## Acknowledgements

This study was supported by Science and Technology Planning Project of Guangdong Province, China (Grant number 2010B060900090).

## Disclosure of conflict of interest

None.

**Address correspondence to:** Qing-Si Zeng, Department of Radiology, The First Affiliated Hospital of Guangzhou Medical University, No. 151, Yan Jiang Road, Yuexiu District, Guangzhou City 510120 Guangdong Province, China. Tel: +86-136-6061-1505; E-mail: qingsizeng@sina.cn

## References

[1] Levitt JE and Matthay MA. Treatment of acute lung injury: historical perspective and potential future therapies. Semin Respir Crit Care Med 2006; 27: 426-437.

[2] Gattinoni L, Pesenti A, Bombino M, Baglioni S, Rivolta M, Rossi F, Rossi G, Fumagalli R, Marcolin R, Mascheroni D and Torresin A. Relationships between lung computed tomographic density, gas exchange, and PEEP in acute respiratory failure. Anesthesiology 1988; 69: 824-832.

[3] Drummond GB. Computed tomography and pulmonary measurements. Br J Anaesth 1988; 80: 665-671.

[4] Malbouisson LM, Muller JC, Constantin JM, Lu Q, Puybasset L and Rouby JJ. Computed to-

mography assessment of positive end-expiratory pressure-induced alveolar recruitment in patients with acute respiratory distress syndrome. Am J Respir Crit Care Med 2001; 163: 1444-1450.
[5] Protti A, Cressoni M, Santini A, Langer T, Mietto C, Febres D, Chierichetti M, Coppola S, Conte G, Gatti S, Leopardi O, Masson S, Lombardi L, Lazzerini M, Rampoldi E, Cadringher P and Gattinoni L. Lung stress and strain during mechanical ventilation: any safe threshold? Am J Respir Crit Care Med 2011; 183: 1354-1362.
[6] Vecchi V, Langer T, Bellomi M, Rampinelli C, Chung KK, Cancio LC, Gattinoni L and Batchinsky AI. Low-dose CT for quantitative analysis in acute respiratory distress syndrome. Crit Care 2013; 17: R183.
[7] Gattinoni L, Caironi P, Cressoni M, Chiumello D, Ranieri VM, Quintel M, Russo S, Patroniti N, Cornejo R and Bugedo G. Lung recruitment in patients with the acute respiratory distress syndrome. N Engl J Med 2006; 354: 1775-1786.
[8] Caironi P, Cressoni M, Chiumello D, Ranieri M, Quintel M, Russo SG, Cornejo R, Bugedo G, Carlesso E, Russo R, Caspani L and Gattinoni L. Lung opening and closing during ventilation of acute respiratory distress syndrome. Am J Respir Crit Care Med 2010; 181: 578-586.
[9] Terragni PP, Rosboch G, Tealdi A, Corno E, Menaldo E, Davini O, Gandini G, Herrmann P, Mascia L, Quintel M, Slutsky AS, Gattinoni L and Ranieri VM. Tidal hyperinflation during low tidal volume ventilation in acute respiratory distress syndrome. Am J Respir Crit Care Med 2007; 175: 160-166.
[10] Desai SR. Acute respiratory distress syndrome: imaging of the injured lung. Clin Radiol 2002; 57: 8-17.
[11] Gattinoni L, Caironi P, Valenza F and Carlesso E. The role of CT-scan studies for the diagnosis and therapy of acute respiratory distress syndrome. Clin Chest Med 2006; 27: 559-570; abstract vii.
[12] Pelosi P, Goldner M, McKibben A, Adams A, Eccher G, Caironi P, Losappio S, Gattinoni L and Marini JJ. Recruitment and derecruitment during acute respiratory failure: an experimental study. Am J Respir Crit Care Med 2001; 164: 122-130.
[13] Henzler D, Mahnken AH, Wildberger JE, Rossaint R, Gunther RW and Kuhlen R. Multislice spiral computed tomography to determine the effects of a recruitment maneuver in experimental lung injury. Eur Radiol 2006; 16: 1351-1359.
[14] Leeman M, Lejeune P and Naeije R. Inhibition of angiotensin-converting enzyme by perindopril diacid in canine oleic acid pulmonary edema. Crit Care Med 1987; 15: 567-573.
[15] Gattinoni L and Cressoni M. Quantitative CT in ARDS: towards a clinical tool? Intensive Care Med 2010; 36: 1803-1804.
[16] Puybasset L, Cluzel P, Gusman P, Grenier P, Preteux F and Rouby JJ. Regional distribution of gas and tissue in acute respiratory distress syndrome. I. Consequences for lung morphology. CT Scan ARDS Study Group. Intensive Care Med 2000; 26: 857-869.
[17] Gattinoni L, Pelosi P, Crotti S and Valenza F. Effects of positive end-expiratory pressure on regional distribution of tidal volume and recruitment in adult respiratory distress syndrome. Am J Respir Crit Care Med 1995; 151: 1807-1814.
[18] Pelosi P, D'Andrea L, Vitale G, Pesenti A and Gattinoni L. Vertical gradient of regional lung inflation in adult respiratory distress syndrome. Am J Respir Crit Care Med 1994; 149: 8-13.
[19] Puybasset L, Rouby JJ, Mourgeon E, Cluzel P, Souhil Z, Law-Koune JD, Stewart T, Devilliers C, Lu Q, Roche S. Factors influencing cardiopulmonary effects of inhaled nitric oxide in acute respiratory failure. Am J Respir Crit Care Med 1995; 152: 318-328.
[20] Matute-Bello G, Frevert CW and Martin TR. Animal models of acute lung injury. Am J Physiol Lung Cell Mol Physiol 2008; 295: L379-399.
[21] Sherr S, Montemurno R and Raffer P. Lipids of recovered pulmonary fat emboli following trauma. J Trauma 1974; 14: 242-246.
[22] Schuster DP. ARDS: clinical lessons from the oleic acid model of acute lung injury. Am J Respir Crit Care Med 1994; 149: 245-260.
[23] Wang HM, Bodenstein M and Markstaller K. Overview of the pathology of three widely used animal models of acute lung injury. Eur Surg Res 2008; 40: 305-316.
[24] Derks CM and Jacobovitz-Derks D. Embolic pneumopathy induced by oleic acid. A systematic morphologic study. Am J Pathol 1977; 87: 143-158.
[25] Hudson LD, Milberg JA, Anardi D and Maunder RJ. Clinical risks for development of the acute respiratory distress syndrome. Am J Respir Crit Care Med 1995; 151: 293-301.
[26] Puybasset L, Gusman P, Muller JC, Cluzel P, Coriat P and Rouby JJ. Regional distribution of gas and tissue in acute respiratory distress syndrome. III. Consequences for the effects of positive end-expiratory pressure. CT Scan ARDS Study Group. Adult Respiratory Distress Syndrome. Intensive Care Med 2000; 26: 1215-1227.
[27] Malbouisson LM, Busch CJ, Puybasset L, Lu Q, Cluzel P and Rouby JJ. Role of the heart in the loss of aeration characterizing lower lobes in acute respiratory distress syndrome. CT Scan ARDS Study Group. Am J Respir Crit Care Med 2000; 161: 2005-2012.

[28] Funama Y, Awai K, Liu D, Oda S, Yanaga Y, Nakaura T, Kawanaka K, Shimamura M and Yamashita Y. Detection of nodules showing ground-glass opacity in the lungs at low-dose multidetector computed tomography: phantom and clinical study. J Comput Assist Tomogr 2009; 33: 49-53.

[29] Lederer DJ, Enright PL, Kawut SM, Hoffman EA, Hunninghake G, van Beek EJ, Austin JH, Jiang R, Lovasi GS and Barr RG. Cigarette smoking is associated with subclinical parenchymal lung disease: the Multi-Ethnic Study of Atherosclerosis (MESA)-lung study. Am J Respir Crit Care Med 2009; 180: 407-414.

[30] Puybasset L, Cluzel P, Chao N, Slutsky AS, Coriat P and Rouby JJ. A computed tomography scan assessment of regional lung volume in acute lung injury. The CT Scan ARDS Study Group. Am J Respir Crit Care Med 1998; 158: 1644-1655.

[31] Chiumello D, Marino A, Brioni M, Menga F, Cigada I, Lazzerini M, Andrisani MC, Biondetti P, Cesana B and Gattinoni L. Visual anatomical lung CT scan assessment of lung recruitability. Intensive Care Med 2013; 39: 66-73.

[32] Caironi P and Gattinoni L. How to monitor lung recruitment in patients with acute lung injury. Curr Opin Crit Care 2007; 13: 338-343.

[33] Tokics L, Strandberg A, Brismar B, Lundquist H and Hedenstierna G. Computerized tomography of the chest and gas exchange measurements during ketamine anaesthesia. Acta Anaesthesiol Scand 1987; 31: 684-692.

[34] Ferguson ND, Fan E, Camporota L, Antonelli M, Anzueto A, Beale R, Brochard L, Brower R, Esteban A, Gattinoni L, Rhodes A, Slutsky AS, Vincent JL, Rubenfeld GD, Thompson BT and Ranieri VM. The Berlin definition of ARDS: an expanded rationale, justification, and supplementary material. Intensive Care Med 2012; 38: 1573-1582.

[35] Ranieri VM, Rubenfeld GD, Thompson BT, Ferguson ND, Caldwell E, Fan E, Camporota L and Slutsky AS. Acute respiratory distress syndrome: the Berlin Definition. JAMA 2012; 307: 2526-2533.

[36] Rouby JJ, Puybasset L, Cluzel P, Richecoeur J, Lu Q and Grenier P. Regional distribution of gas and tissue in acute respiratory distress syndrome. II. Physiological correlations and definition of an ARDS Severity Score. CT Scan ARDS Study Group. Intensive Care Med 2000; 26: 1046-1056.

**Supplemental Table 1.** Comparison of CT HUs, residual volume, tissue weight, and percentage of lung areas for ARDS vs. controls

| | | Expiratory phase | | | | | Inspiratory phase | | | | |
|---|---|---|---|---|---|---|---|---|---|---|---|
| | | ARDS | | Control | | *P*-value | ARDS | | Control | | *P*-value |
| | | Mean | SD | Mean | SD | | Mean | SD | Mean | SD | |
| CT (HU) | T0 | -670.62 | 54.57 | -677.88 | 26.97 | 0.807 | -861.86 | 10.49 | -856.51 | 11.54 | 0.416 |
| | T1 | -618.34 | 118.97 | -686.37 | 24.92 | 0.290 | -842.32 | 43.77 | -853.46 | 9.70 | 0.631 |
| | T2 | -578.30 | 149.24 | -676.73 | 32.65 | 0.226 | -824.30 | 52.22 | -854.05 | 11.51 | 0.292 |
| | T3 | -567.47 | 114.14 | -689.36 | 39.12 | 0.063 | -810.88 | 49.54 | -856.20 | 11.55 | 0.102 |
| | T4 | -538.19 | 109.82 | -670.23 | 46.76 | 0.042 | -782.78 | 69.44 | -845.75 | 19.11 | 0.106 |
| | T5 | -507.42 | 117.25 | -675.07 | 59.79 | 0.020 | -756.24 | 66.00 | -828.79 | 22.87 | 0.057 |
| | T6 | -391.35 | 135.46 | -627.48 | 50.71 | 0.000 | -659.63 | 63.32 | -750.37 | 46.85 | 0.024 |
| Normally aerated area (%) | T0 | 77.67 | 5.53 | 79.24 | 2.39 | 0.600 | 46.61 | 8.80 | 50.37 | 10.83 | 0.509 |
| | T1 | 72.03 | 17.67 | 83.33 | 1.46 | 0.236 | 54.58 | 12.38 | 54.34 | 10.27 | 0.974 |
| | T2 | 67.24 | 20.19 | 81.24 | 2.35 | 0.202 | 64.35 | 12.49 | 56.80 | 11.03 | 0.314 |
| | T3 | 66.32 | 12.76 | 80.93 | 3.05 | 0.047 | 68.75 | 11.38 | 50.48 | 11.09 | 0.018 |
| | T4 | 59.29 | 14.45 | 72.71 | 8.65 | 0.112 | 61.72 | 12.77 | 47.61 | 11.44 | 0.080 |
| | T5 | 52.20 | 17.99 | 69.57 | 8.16 | 0.093 | 51.87 | 21.43 | 43.34 | 17.79 | 0.497 |
| | T6 | 33.17 | 15.65 | 50.45 | 13.75 | 0.079 | 32.30 | 18.58 | 25.07 | 14.35 | 0.501 |
| Non-aerated lung area (%) | T0 | 2.01 | 0.96 | 1.61 | 0.24 | 0.434 | 0.77 | 0.18 | 0.75 | 0.19 | 0.830 |
| | T1 | 2.26 | 0.86 | 1.03 | 0.15 | 0.017 | 1.10 | 1.13 | 0.69 | 0.13 | 0.489 |
| | T2 | 3.52 | 1.89 | 1.13 | 0.18 | 0.030 | 0.91 | 0.51 | 0.59 | 0.13 | 0.245 |
| | T3 | 4.56 | 2.23 | 1.48 | 0.77 | 0.021 | 0.96 | 0.29 | 0.79 | 0.16 | 0.284 |
| | T4 | 5.69 | 3.62 | 1.54 | 0.83 | 0.047 | 1.18 | 0.66 | 0.76 | 0.20 | 0.235 |
| | T5 | 6.90 | 4.63 | 1.65 | 0.86 | 0.006 | 1.31 | 0.70 | 0.83 | 0.17 | 0.204 |
| | T6 | 16.39 | 10.88 | 3.39 | 0.67 | 0.004 | 3.40 | 1.75 | 2.67 | 1.12 | 0.457 |
| Poorly aerated area (%) | T0 | 14.80 | 5.87 | 13.41 | 1.85 | 0.659 | 2.30 | 0.30 | 2.40 | 0.20 | 0.559 |
| | T1 | 19.03 | 10.70 | 10.61 | 2.48 | 0.154 | 2.80 | 1.59 | 2.43 | 0.30 | 0.656 |
| | T2 | 20.71 | 7.38 | 12.97 | 4.34 | 0.077 | 3.10 | 2.33 | 2.13 | 0.06 | 0.433 |
| | T3 | 23.76 | 9.92 | 11.32 | 3.58 | 0.034 | 3.56 | 2.36 | 2.41 | 0.24 | 0.360 |
| | T4 | 27.05 | 11.99 | 13.66 | 4.48 | 0.054 | 4.04 | 2.00 | 2.66 | 0.21 | 0.059 |
| | T5 | 28.98 | 11.65 | 15.23 | 5.21 | 0.045 | 4.36 | 2.11 | 2.75 | 0.25 | 0.040 |
| | T6 | 38.32 | 13.13 | 27.97 | 9.22 | 0.179 | 8.93 | 6.42 | 5.16 | 0.32 | 0.274 |
| Hyper-aerated area (%) | T0 | 5.38 | 3.95 | 5.00 | 3.10 | 0.866 | 48.27 | 8.12 | 45.05 | 9.90 | 0.538 |
| | T1 | 3.63 | 2.72 | 4.52 | 2.07 | 0.573 | 39.85 | 13.59 | 40.94 | 8.78 | 0.886 |
| | T2 | 3.21 | 2.74 | 4.01 | 2.28 | 0.621 | 30.25 | 13.67 | 39.02 | 10.21 | 0.273 |
| | T3 | 2.66 | 2.49 | 5.49 | 4.65 | 0.157 | 25.38 | 12.96 | 44.46 | 9.98 | 0.022 |
| | T4 | 2.60 | 2.44 | 4.86 | 2.33 | 0.140 | 24.10 | 11.82 | 47.47 | 9.31 | 0.004 |
| | T5 | 3.72 | 3.02 | 5.42 | 2.97 | 0.357 | 32.17 | 16.76 | 50.07 | 9.05 | 0.027 |
| | T6 | 8.31 | 7.97 | 7.93 | 4.67 | 0.931 | 50.75 | 14.34 | 59.67 | 11.00 | 0.289 |
| Residual volume (ml) | T0 | 363.55 | 110.01 | 383.63 | 59.84 | 0.740 | 1265.97 | 201.89 | 1201.56 | 197.62 | 0.598 |
| | T1 | 326.78 | 97.80 | 388.29 | 59.76 | 0.269 | 1190.02 | 230.94 | 1184.33 | 229.00 | 0.967 |
| | T2 | 325.43 | 127.48 | 373.95 | 46.91 | 0.481 | 1164.00 | 227.17 | 1125.03 | 178.69 | 0.766 |
| | T3 | 333.73 | 114.96 | 376.76 | 82.60 | 0.513 | 1212.07 | 212.43 | 1157.84 | 185.43 | 0.664 |
| | T4 | 332.83 | 108.64 | 392.85 | 81.10 | 0.342 | 1251.21 | 165.22 | 1149.01 | 167.31 | 0.318 |
| | T5 | 356.77 | 106.33 | 396.87 | 83.83 | 0.516 | 1291.05 | 203.81 | 1164.23 | 182.89 | 0.302 |
| | T6 | 430.27 | 130.52 | 480.85 | 77.32 | 0.488 | 1533.05 | 135.80 | 1341.06 | 242.19 | 0.079 |
| Tissue weight (g) | T0 | 167.21 | 18.54 | 180.54 | 19.64 | 0.255 | 201.21 | 23.04 | 199.16 | 18.03 | 0.877 |
| | T1 | 195.29 | 51.41 | 176.41 | 24.03 | 0.502 | 218.39 | 53.32 | 201.08 | 23.35 | 0.550 |
| | T2 | 225.70 | 64.68 | 177.53 | 19.69 | 0.178 | 244.08 | 70.72 | 191.96 | 32.47 | 0.190 |
| | T3 | 252.80 | 70.20 | 159.82 | 7.56 | 0.024 | 278.12 | 65.07 | 192.42 | 16.60 | 0.003 |
| | T4 | 273.46 | 72.07 | 178.19 | 22.42 | 0.026 | 309.11 | 81.28 | 196.72 | 29.26 | 0.021 |
| | T5 | 293.88 | 79.79 | 188.26 | 26.09 | 0.026 | 347.15 | 82.08 | 209.41 | 37.28 | 0.008 |
| | T6 | 408.51 | 72.92 | 260.41 | 62.79 | 0.004 | 466.60 | 107.01 | 288.93 | 82.33 | 0.012 |